DISCOVERING THE ROLE OF AUTOINHIBITION IN KINETICS HETEROGENEITY OF EVOKED DOPAMINE RESPONSES

by

Han-Chen Wu

B.S. Chemistry; B.A. Biochemistry, University of Washington, 2013

Submitted to the Graduate Faculty of

the Kenneth P. Dietrich School of Arts and Sciences in partial fulfillment

of the requirements for the degree of

Master of Science

University of Pittsburgh

2017

UNIVERSITY OF PITTSBURGH

DIETRICH SCHOOL OF ARTS AND SCIENCES

This thesis was presented

by

Han-Chen Wu

It was defended on

November 15, 2016

and approved by

Shigeru Amemiya, Associate Professor, Department of Chemistry

Renã A.S. Robinson, Assistant Professor, Department of Chemistry

Committee Chair: Adrian C. Michael, Professor, Department of Chemistry

Adrian C. Michael

DISCOVERING THE ROLE OF AUTOINHIBITION IN KINETICS HETEROGENEITY OF EVOKED DOPAMINE RESPONSES

Han-Chen Wu, M.S.

University of Pittsburgh, 2017

Dopamine (DA) contributes to critical functions in the central nervous system. By introducing electrical stimulation *in vivo* at the rat's medial forebrain bundle, evoked DA signals can be measured at a carbon fiber electrode with fast scan cyclic voltammetry (FSCV) in rat's dorsal striatum. Previously, evidence suggested that the heterogeneity in evoked DA responses reflects the difference in inherent kinetics, which might play an important role physiologically.

A restricted diffusion based numerical model produced great fit between simulations and observed responses for stimulation lengths no longer than 3 seconds, using 4 or sometimes 3 adjustable parameters. A study was designed to explore different supra-physiological stimuli and examine these evoked responses in the dorsal striatum after raclopride, a D2 antagonist drug, was given. The effects of raclopride were different based on the kinetic heterogeneity, and a refined DA kinetic model was used to model the responses up to stimulation lengths of 10 seconds. Based on the new model, it seems that the domains are different in autoinhibitory tone, which derives from different basal DA concentration required to activate the D2 receptors.

The parameters can be used to generate delivery and clearance curves that represent the DA being delivered to and cleared from the electrode at each time point. Often, multiple parameters sets will produce good fits to individual evoked responses. In these cases, however, the multiple parameter sets generate similar delivery and clearance curves. For this reason, we conclude that delivery and clearance curves provide an effective tool for investigating the kinetic properties of DA systems.

TABLE OF CONTENTS

LIST OF TABLES

LIST OF FIGURES

LIST OF EQUATIONS

1.0 INTRODUCTION

1.1 NIGROSTRIATAL DOPAMINE PATHWAY

Dopamine (DA) is one of the most important neurotransmitters in the central nervous system (CNS). DA contributes to many critical functions such as reward mechanisms, learning and motor control (Double and Crocker, 1995; Reynolds et al., 2001; Schultz, 2002). Any type of abnormality in the DA system could lead to disorders including schizophrenia, Parkinson's disease and drug addiction (Grace, 1995; Lotharius et al., 2002; Pappatà et al., 2008).

In the nigrostriatal pathway, the cell body of DA neuron is in the substantia nigra, where it extends its axon through medial forebrain bundle (MFB) and terminates in the striatum (Carr and White, 1986; Horvitz, 2000). The neurons usually maintain a voltage difference across the cell's membrane, with a resting potential lower than the potential of extracellular space. When a synaptic input causes the potential to rise above the threshold, an action potential is produced by voltage gated ion channels. This causes the sodium (Na^+) channels to open and allow Na^+ to flow into the cell, following by potassium (K^+) channels opening which allow K^+ to flow out and create an outward current. The influx of Na^+ depolarizes the cell while the efflux of K^+ repolarizes the cell, bringing the membrane potential back to its resting potential (Nelson, 2004). Upon the arrival of an action potential, the calcium ion (Ca^{2+}) channels are opened, causing an increase in the Ca^{2+} concentration inside the cell (Ceccarelli and Hurlbut, 1980). The influx of

Ca^{2+} causes the vesicles containing dopamine to fuse to presynaptic cell membrane and release dopamine into synaptic gap with calcium ions acting as a second messenger.

DA is synthesized first by converting L-tyrosine to L-3,4-dihydroxyphenylalanine (L-DOPA) and then from L-DOPA into DA by DOPA decarboxylase (Elsworth and Roth, 1997). Once synthesized, it is then packaged into vesicles. The interaction between DA and the targeted protein receptors allows the presynaptic neuron to communicate with the postsynaptic cell. These receptors are G-protein coupled receptors (GPCR) made up of seven alpha helices that span throughout the cell membrane. When DA is bound on their extracellular side, the receptor changes its conformation in the cytoplasmic side and alters the binding affinity of the G-protein to the receptor. After DA is bound to the receptor, the G-protein complex dissociates from the receptor. There are two main types of DA receptors; D1-like receptors activate adenylate cyclase (AC) and increase intracellular levels of cyclic adenosine monophosphate (cAMP) while D2-like receptors inhibit AC and decrease the production of cAMP (Onali et al., 1985; Missale et al., 1998; Ford, 2014). The postsynaptic cells contain both D1 and D2-like receptors and the presynaptic terminals only have D2-like receptors (Delle Donne et al., 1997). DA released from neuron terminals elevates the extracellular DA concentration activating the receptor protein.

Clearance of DA is accomplished via the dopamine transporter (DAT) (Benoit-Marand et al., 2000; Salahpour et al., 2008). It is an integral membrane protein symporter that removes DA back to the cytosol by coupling its movement with Na^+/K^+ ATPase. By co-transporting two Na^+ ions and one Cl^- ion, the created ion concentration gradient allows the reuptake of DA (Torres et al., 2003). DAT decreases the extracellular DA concentration, terminating the activation of the transmembrane receptor proteins.

.

1.2 IN VIVO ELECTROCHEMICAL DETECTION OF DOPAMINE

Dopamine is an electroactive catecholamine with two hydroxyl groups on the benzene ring. DA can be oxidized by removing two electrons and two protons, converting into dopamine-o-quinone (DAQ) (Figure 1). The process is reversible, which allows DAQ to be reduced to DA by adding back two electrons and two protons. However, since the oxidation and reduction of the two electrons and two protons are occuring as four separate events, there are six possible pathways known as the nine-member box (Wipf et al., 1986). Because the oxidation and reduction go through different pathways, the separation of oxidation and reduction peaks is larger than the 29.5 mV predicted by the ideal reversible reaction (Bard and Faulkner, 2001).

Micro carbon fiber electrodes (CFE) are most commonly used for DA detection (Figure 2). The CFE is 5-7 μm in diameter so it is small enough to minimize tissue damage while sampling *in vivo* (Jaquins-Gerstl and Michael, 2009) and allows high spatial resolution (Kile et al., 2012). The small surface area of the electrode limits the number of terminals from which it samples. Thus, the CFE measures DA responses from a discrete population of terminals unlike microdialysis, another sampling technique (Michael et al., 2005; Nesbitt et al., 2013). The CFE has a high sensitivity to the change in DA concentration and has a detection limit in the nM ranges.

The potential required for the oxidation-reduction reaction depends on the scan rate; the voltammogram contains information such as shape of the curve, peak height and peak separation that can serve as the “fingerprint” of the analyte. Also, the magnitude of the current can be converted to the change in concentration via a simple calibration curve. Due to these properties, an incredible amount of information can be gathered from fast scan cyclic voltammetry (FSCV). With a scan rate of 400 V/s, FSCV is able to complete the 3 V scan in 7.5 ms (Figure 3), giving

it sub-second temporal resolution (Missale et al., 1998; Bath et al., 2000). The fast scan rate also eliminates other interference that has similar oxidation and reduction potentials to DA because those reactions are slower. Taken together, FSCV with CFE detection is capable of detecting sub-second, high nM concentration changes from a small population of neurons *in vivo*.

However, FSCV method is not suitable to measure the baseline concentration of an analyte. The main source of the total signal is from the non-faradaic charging current caused by the fast scan rate. Furthermore, the amplitude of the background current depends on the experimental setup, buffer solution and electrode. Therefore, it is impossible to measure DA from a single FSCV voltammogram; at least a background scan before the DA concentration changes and a scan following the change are both required (Figure 4). Because of the large charging current, FSCV is used to measure the change in DA concentration instead of its basal level. The magnitude of change is independent to the baseline DA concentration present within the limits of detection.

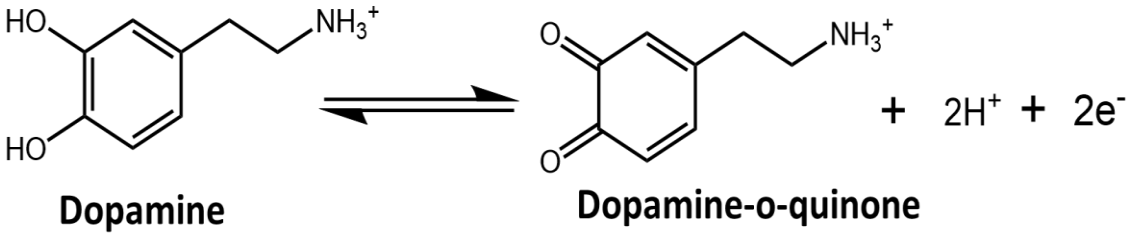

Figure 1 Oxidation and reduction process of dopamine.

Dopamine is being oxidized to dopamine-o-quinone and being reduced back to dopamine. This reversible reaction involves 2 electrons and 2 protons and is governed by the nine-member box scheme (Wipf et al., 1986).

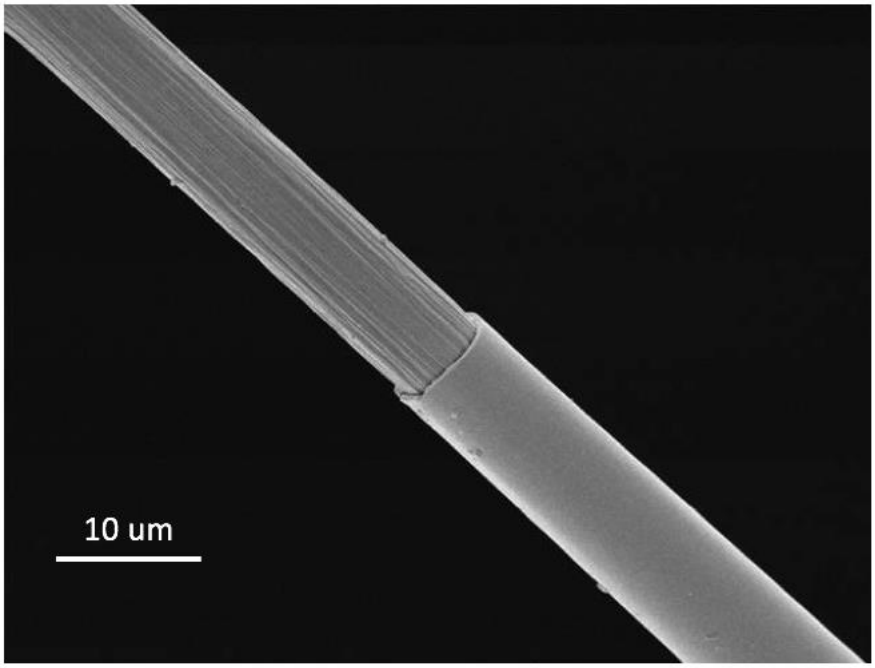

Figure 2 Electron microscopy image of carbon fiber microelectrode.

The carbon fiber electrode is around 5-7 μm in diameter and is cut to the length of 250 μm. The glass capillary is pulled to a tight tip around the carbon fiber then sealed with slurry epoxy to secure it.

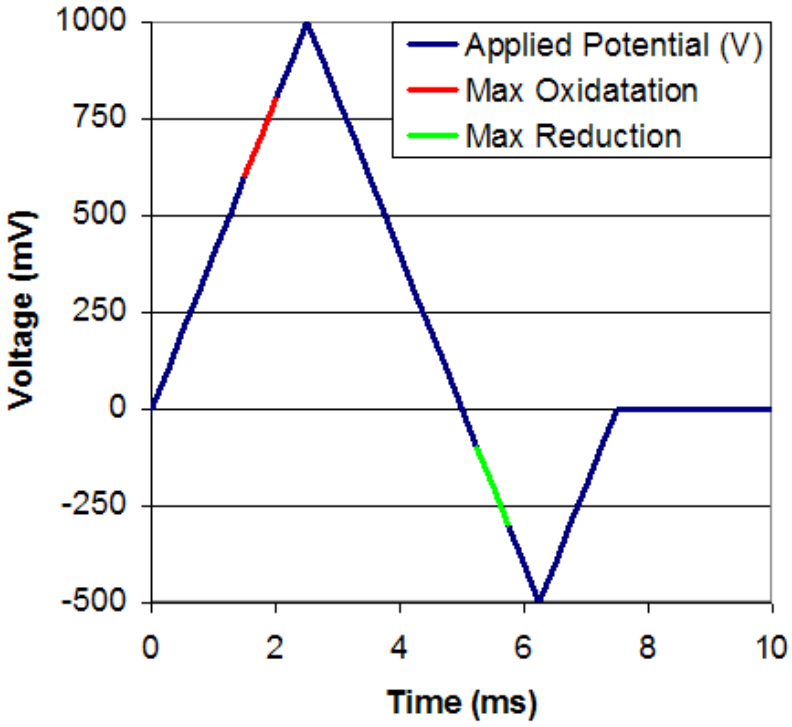

Figure 3 Fast scan cyclic voltammetry scan.

The potential was held at 0 V, ramping up to 1 V at a scan rate of 400 V/s, scanning down to -0.5 V, and back to 0 V versus Ag/AgCl. The entire scan was finished within 7.5 ms, which gives sub-second temporal resolution. Red line is where oxidation reaction happens and green line is where reduction happens.

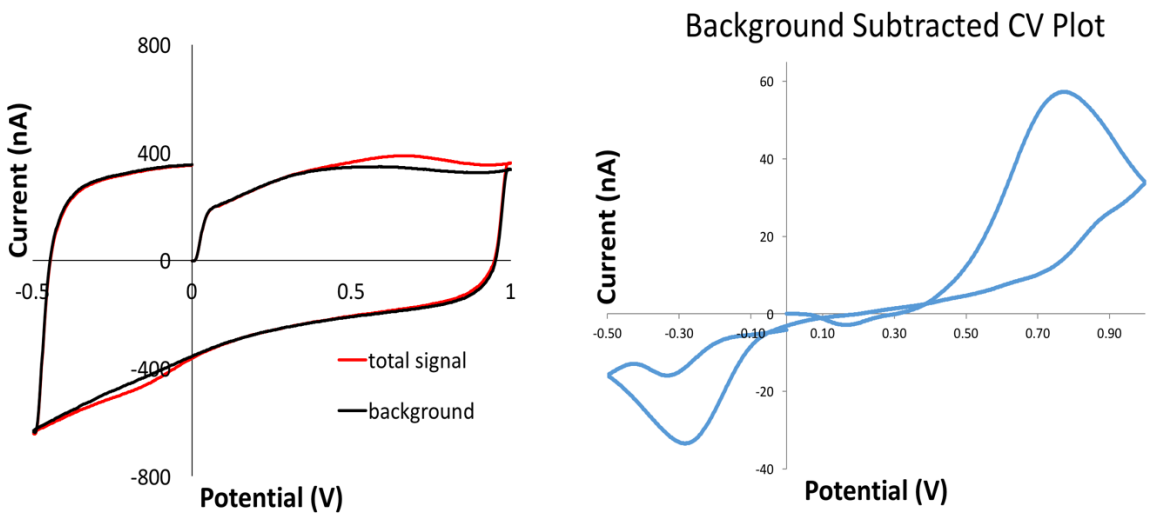

Figure 4 Cyclic voltammogram of fast scan cyclic voltammetry.

Before (left) and after (right) background subtraction. Charging current (black line) contributes to the major part of to the total signal (red line). Therefore, the background should be subtracted in order to see the current generated due to the change in DA.

2.0 METHOD AND MATERIAL

2.1 VOLTAMMETRY

Borosilicate capillaries (0.58 mm I.D., 1.0 mm O.D., Sutter Instruments, Novato, CA) were soaked in acetone overnight. Carbon fiber electrodes were made by pulling cleaned and dried glass capillaries to sharp tips around a single carbon fiber (7 μm in diameter, T650, Cytec Carbon Fibers LLC., Piedmont, SC) with a vertical glass puller (Narishige, Tokyo, Japan). The tips were sealed with Spurr Epoxy (Polysciences Inc., Warrington, PA) and cured in oven at 70 ºC overnight. Carbon fibers extending from the seal were trimmed under the microscope to 250 μm in length. Microelectrodes were pre-treated by soaking the tip in isopropyl alcohol (Sigma Aldrich, St. Louis, MO) containing activated carbon powder (Fisher Scientific, Pittsburgh, PA) for at least 30 minutes prior to the experiment.

FSCV was performed with a computer controlled potentiostat (EI-400, Ensman Instruments, Bloomington, IN) and CV Tarheels software (Version 4.3, courtesy of Dr. Michael Heien, University of Arizona, Tucson, AZ). The potential was held at a resting potential of 0 V, ramped at a scan rate of 400 V/s from 0 V to 1 V, down to -0.5 V and back to 0 V versus a Ag/AgCl reference electrode. Scans were performed at 10 Hz (Figure 5). Dopamine voltammograms were obtained by background subtraction.

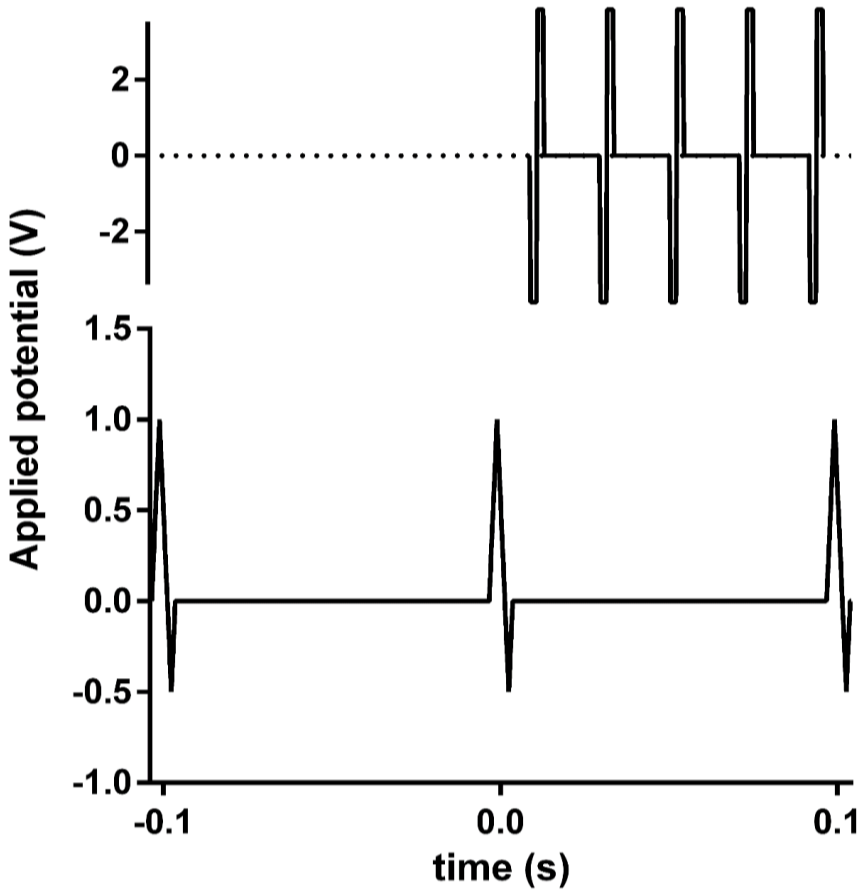

Figure 5 FSCV waveform and stimulus pulses.

The FSCV waveform and stimulus pulse are offset in time so they do not overlap. The waveform is applied at a frequency of 10 Hz. The stimulus is a 2 ms biphasic pulse with pulse height of 250 μA at a frequency of 60 Hz by optically isolated stimulus boxes.

2.2 ELECTRODE CALIBRATION

The electrodes are calibrated *in vitro* to establish the relationship between current and DA concentration. The calibration is both carried out pre- and post-experiment in a flow cell with gravity fed nitrogen purged artificial cerebral spinal fluid (aCSF: 152 mM Cl^-, 145 mM Na^+, 2.7 mM K^+, 1.2 mM Ca^+, 2.0 mM phosphate, pH 7.4). Standards for calibration were prepared by dissolving dopamine hydrochloride (Sigma Aldrich, St. Louis, MO) in aCSF. Conversion of *in vivo* oxidation currents to DA concentration conversion was based on post-calibration results.

2.3 ANIMALS AND SURGICAL PROCEDURES

All *in vivo* animal procedures were performed under approval of the Institutional Animal Care and Use of Committee (IACUC) of the University of Pittsburgh. Male Sprague-Dawley rats (250-350 g) (Charles River, Raleigh, NC) were intubated then anesthetized with isoflurane (2% by volume, Baxter Healthcare, Deerfield, IL) and placed in a stereotaxic frame (David Kopf Instruments, Tujunga, CA) and wrapped in a heating blanket (Harvard Apparatus, Holliston, MA) that kept the body temperature at 37 °C. The scalp was shaved and the skull was exposed. Three holes were drilled through the skull. The dura was carefully removed to expose the brain. The incisor bar was adjusted so that the dorsal ventral measurements at lambda and bregma were no more than 0.01 mm apart (flat skull).

Electrical connection between the brain and the reference electrode was established by creating a salt bridge with a Kimwipe soaked in aCSF held together with a plastic pipette tip. A carbon fiber microelectrode was placed in the ipsilateral striatum (from bregma: 3.8 mm lateral,

0.2 mm anterior, 4.5 mm below dura) using a stereoscope to avoid hitting any surface blood vessels. A bipolar, stainless steel stimulating electrode (MS 303-1-untwisted, Plastics One, Roanoke, VA) was lowered into the ipsilateral medial forebrain bundle (MFB, from midline: 1.2 mm lateral, from bregma: 4.3 mm posterior, 7.2 mm below dura). The final position was set by lowering the microelectrode until evoked DA release was observed in the striatum. The relative positions can be seen in figure 6 and figure 7.

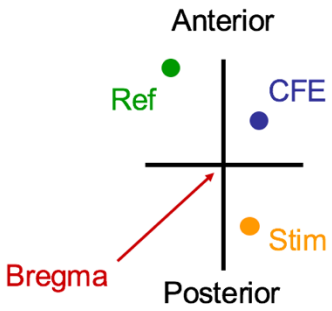

Figure 6 Relative positions looking from the top.

The relative potions of reference electrode, carbon fiber electrode and stimulating electrode relative to bregma.

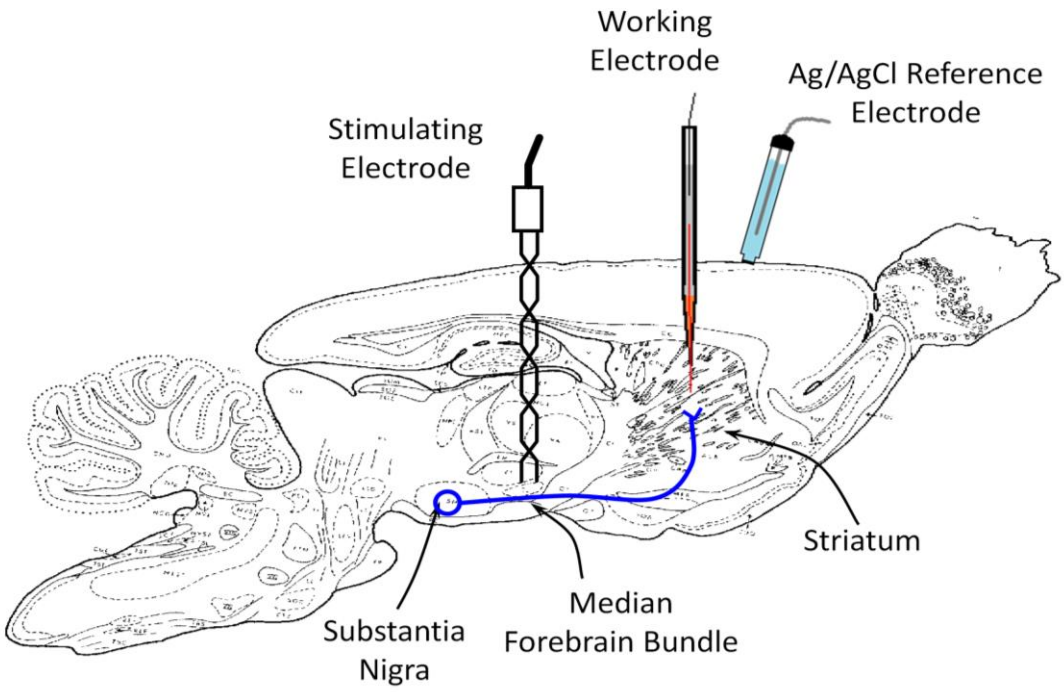

Figure 7 Sagittal view of the experimental setup.

The reference electrode is placed in contact with the brain, the working electrode is placed in striatum, and the stimulating electrode is lowered into the MFB.

3.0 INTRODUCTION AND MOTIVATION

3.1 THE HETEROGENEITY OF DOPAMINE RESPONSES

The long-known explanation of heterogeniety of DA releases has been attributed to the difference in terminal density in the striatum. It was thought that some recording sites are closer to the electrode (Garris et al., 1994). The hypothesis suggests that different gap sizes between the terminals and the electrode result from differing terminal desnities. For responses that require stimulations longer than 0.2s to be observed, it implied that DA has to diffuse across the larger gap between the terminals and the electrodes for the signal to be detected. As a result, it has been common practice to optimize the position of CFE to sites with high population of DA terminals for the responses to be seen quickly upon stimulation. The non-optimized responses have been concluded to the electrode being in an area away from DA terminals (Peters and Michael, 2000).

However, we were able to demonstrate that the heterogeneity of dopamine responses is due to kinetics (Moquin and Michael, 2009). The responses were widely separated into fast and slow responses (Figure 8). Fast sites respond immediately to stimulation, as little as 0.2 seconds, while it can take longer than 0.2 seconds for slow sites to respond (Moquin and Michael, 2009). Fast sites can be further categorized into four subtypes. In short, type 1 fast sites are linear for the entire duration of stimulus, type 2 increase continuously but not in a linear fashion, type 3 do not

increase during the entire stimulation and are non-linear, and type 4 are biphasic. The fast sites being focused in this entire document are type 4 responses because this type of responses reveal the simultaneous detection of DA from terminals exhibiting heterogeneous behaviors within one single recording. This is also why type 4 responses are usually referred as hybrid responses (Figure 9).

Fast and slow sites responses respond differently to D2 antagonists. It is hypothesized that the slow responses result from autoinhibition, which exists prior to the stimulus, presumably due to basal DA in the extracellular space being sufficient to activate the pre-synaptic D2 receptors (Usiello et al., 2000; Benoit-Marand et al., 2001; Kita et al., 2007). Raclopride, a D2 antagonist, increases evoked DA release upon prolonged electrical stimulation (longer than 200 ms) but does not effect responses from short stimuli (1~4 pulses at 60Hz) (Garris et al., 1994). The absense of an effect on brief stimulus responses implies a minimal of autoinhibition for fast sites.

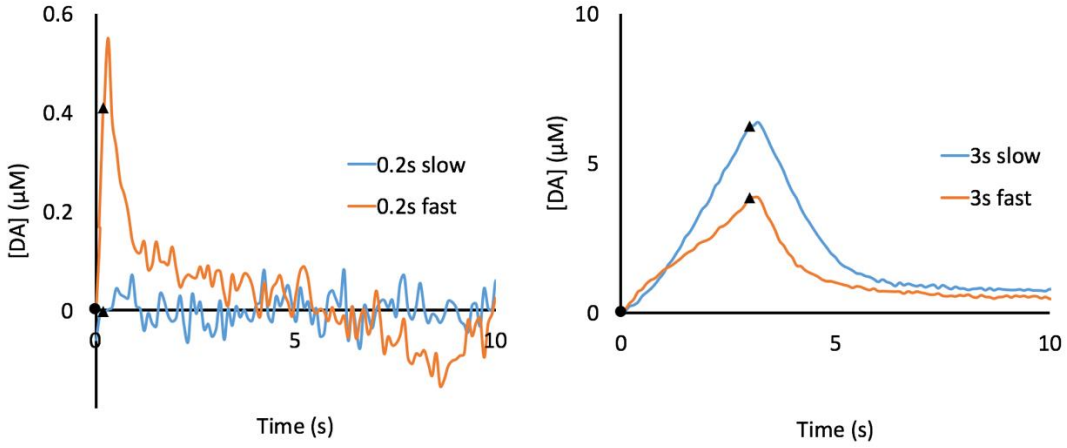

Figure 8 Fast and slow type evoked responses.

In Fast sites, DA is detected immediately upon the first 0.2 s of stimulation while slow sites require longer than 0.2 s for DA to be detected (left, 0.2 s stimulation length). Slow site responses can be detected with longer stimulation (right, 3 s stimulation length). Circles indicate the start of the stimulation and triangles indicate the end of stimulation.

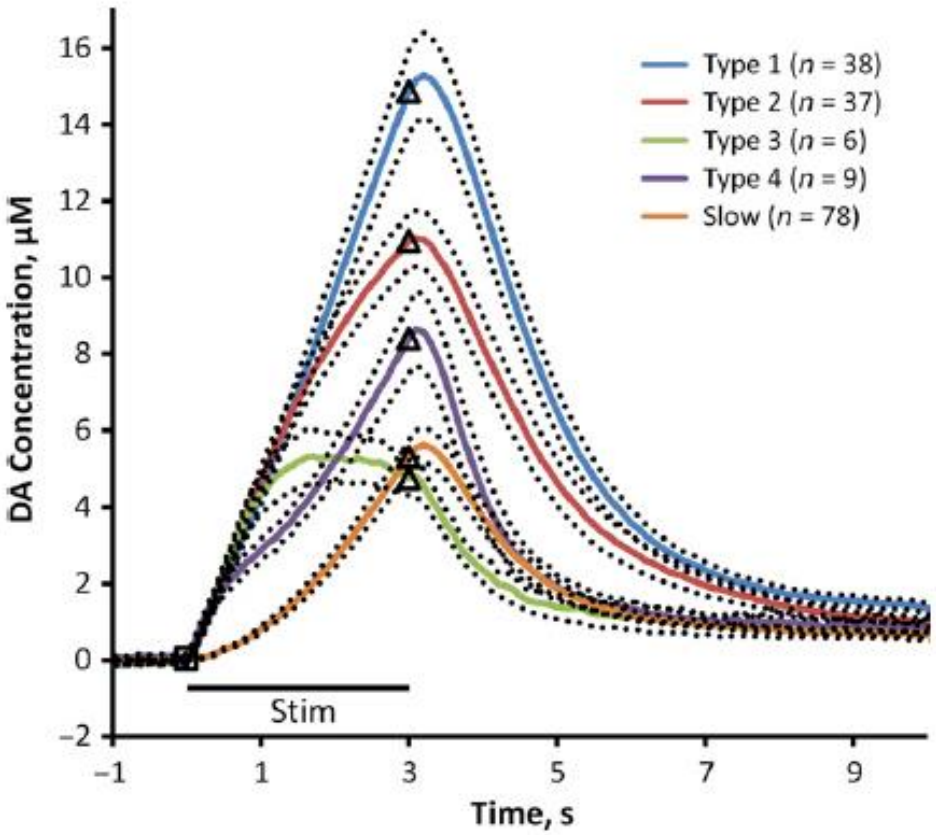

Figure 9 The five dorsal striatum responses.

Fast site responses are categorized into 4 types, where type 4 is also called a hybrid type. The square is the start of stimulus and triangles are the ends of the stimulus. Solid lines are the average of responses and dotted lines are the SEMs (Figure taken from Taylor et al., 2015).

3.2 MODELING THE IN VIVO DOPAMINE KINETICS

The Diffusion Gap (DG) model was the reigning explanation of the heterogeneous kinetics of DA. This model proposes that there is a physical gap between the DA terminal and the recording site (Wightman et al., 1988). The theory proposed that the slow response was the effect of CFE placed a certain distance from the DA terminals. During an electrical stimulation, DA is immediately released but it requires some time to diffuse to the electrode, which causes a delay in the signal (Venton et al., 2003). This hypothesis implies that the slow responses are caused by experimental errors and poor choice of recording sites (Wu et al., 2001).

However, there are several problems with this model. For example, a lag happens when the response doesn't immediately take off upon stimulation and an overshoot happens when the signal continues to rise even after the stimulus ends. According to this model, response with lag should be accompanied with overshoot, but this is not always the case. The duration of lag and overshoot should be the same, however this is not always observed. In addition, raclopride can eliminate the delay in the onset of the DA signal observed in a slow site. There cannot be a physical gap between the recording site and the DA terminals because pharmacological conditions should not change the physical properties of the space.

An alternate explanation was introduced by our lab based on the concept of restricted diffusion (RD). The original RD model can be represented by equations 1 and 2 (Walters et al., 2014):

$$\frac{dDA_{ic}}{dt} = R_p f\text{-}DA_{ic} k_T$$

Equation 1

$$\frac{d[DA]_{oc}}{dt} = \frac{DA_{ic}k_T}{V_{oc}} - [DA]_{oc}k_U$$

Equation 2

Where this mechanism hypothesizes that DA molecules cannot diffuse freely throughout the extracellular space. The extracellular space is divided into an inner compartment (IC) and an outer compartment (OC) space to describe the delay in the DA transport. DA is released per stimulus pulse, *Rp*, from axon terminals to the IC then transported to the electrode via a first order transport rate k_T. DA is detected in the OC by FSCV and the uptake from the OC back to the vesicles can be represented by first order rate k_U. The detected DA concentration is represented by the term $[DA]_{oc}$ with V_{oc} as the volume of the OC and f as the stimulation frequency.

A fourth parameter k_R was introduced as an exponential release modulator as it better represents the curvature of increase in amplitude during the stimulus in both fast and slow sites (Walters et al., 2015). The refined four parameter RD model is shown below (Walters et al., 2015):

$$\frac{dDA_{ic}}{dt} = R_p f e^{-k_R t} - DA_{ic}k_T$$

Equation 3

The addition of k_R allows the responses to be more accurately reproduced with the model. It reflects the data better than a constant addition of DA. By modeling responses obtained with high-pulse stimuli, the RD model reveals new information about the kinetics of the fast and slow kinetic domains (Walters et al., 2014, 2015, 2016).

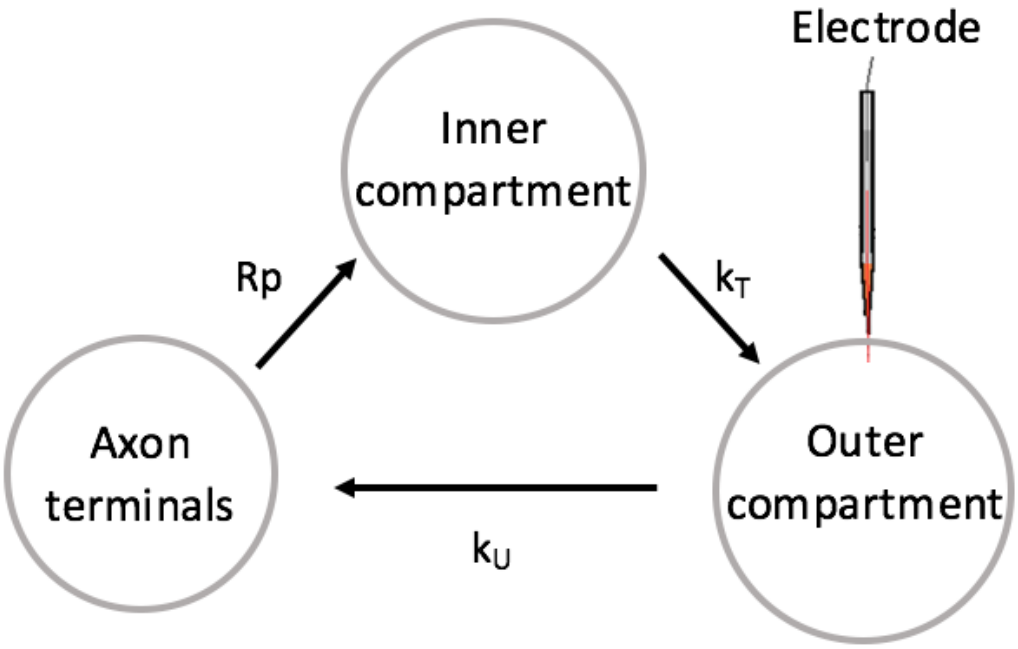

Figure 10 Restricted diffusion (RD) model.

A constant amount of DA is released per stimulus pulse by *Rp* from the axon terminals to the inner compartment (IC). DA is then transported at a first order rate k_T to the outer compartment (OC), where the DA is detected by the electrode. At last, DA in the outer compartment is removed by a first order uptake rate k_U back to the terminals. The release of DA is modulated by k_R (which is not portrayed in this figure).

3.3 BI-EXPONENTIAL MODEL—5 PARAMETERS

The RD model is not sufficient to describe stimulations of longer length, illustrated in figure 3.4(a) as a 10 second, 60 Hz stimulation. In these cases, the DA concentration does not increase during the entire length of the stimulation; it increases to a certain degree then starts to decrease until the stimulus ends. In this specific case, a fifth parameter, k_{R2}, is also used to modulate DA release into the inner compartment as follows:

$$\frac{dDA_{ic}}{dt} = R_p f(e^{-k_{R1}t} - e^{-k_{R2}t}) - DA_{ic}k_T$$

Equation 4

Where DA_{ic} is the amount of DA in moles in the inner compartment, R_p is the moles of DA released per stimulus pulse, k_{R1} and k_{R2} are first-order rate constants that modulates DA release over time, and k_T is the first-order transport rate constant. f is the stimulus frequency, which is held constant. This equation, a modified version of the inner compartment component of the RD model equation described above, is referred to here as the biexponential version of the RD model. As shown in figure 3.4, the bi-exponential model can reproduce data from longer stimulations much more accurately ($r^2 > 0.9994$) than the four parameter RD model ($r^2 > 0.9931$). The bi-exponential model allows longer responses, up to 20 seconds, to be fitted. With the bi-exponential model, we can further study the slow components of evoked responses that were long neglected.

(A)

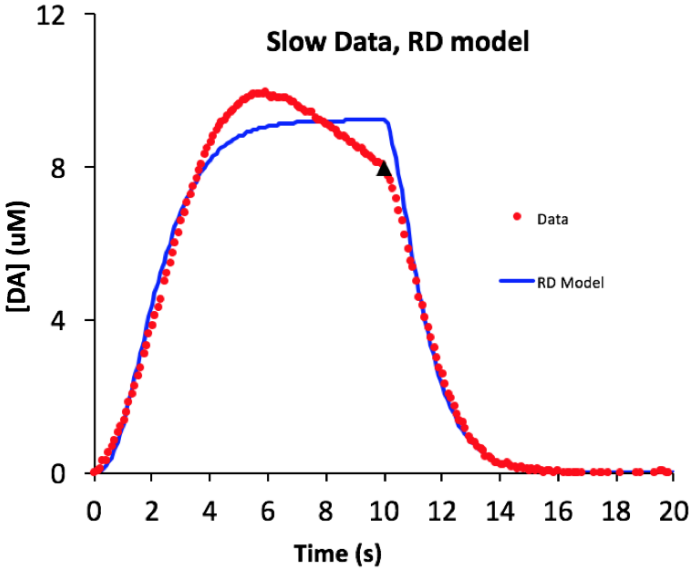

(B)

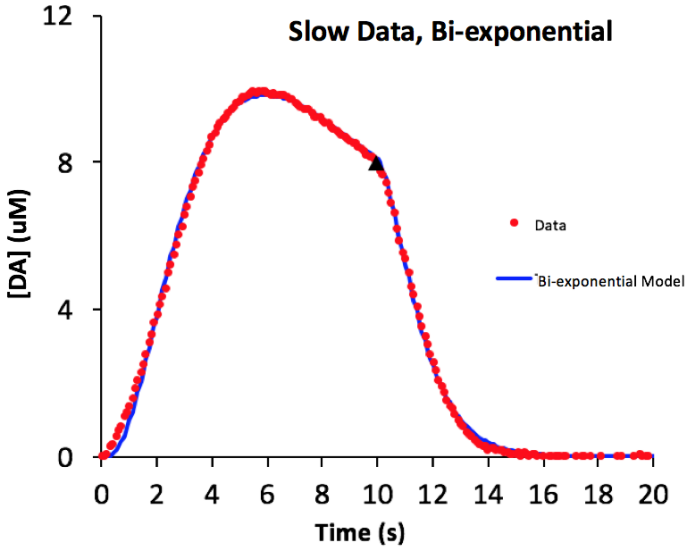

Figure 11 (A) RD model fit (B) Bi-exponential model fit.

The evoked responses (frequency = 60 Hz, stimulation length = 10 seconds) are averaged of n=7 slow site rats in both cases with model fits. SEMs neglected for sake of clarity. The bi-exponential model can produce a much better fit.

3.4 MOTIVATION

Previously, our lab's findings suggested that there are different tonic basal DA concentrations present in extracellular space. This supports the idea that the slow domains are due to a sufficient pre-stimulus DA concentration which activates the pre-synaptic D2 autoreceptors, however this phenomena is absent in fast domains (Moquin and Michael, 2009; Wang et al., 2010). Such different results are due to the heterogeneity of the evoked DA kinetics. While autoinhibition can be caused by pre-stimulus DA concentrations, it can also be caused by long stimulation lengths resulting in post-stimulus autoinhibition. However, at present, it is unclear if such differences are caused by pre-stimulus autoinhibition because we were not able to model longer evoked DA responses. Therefore, the goal of this study was to examine DA responses in both domains with the new bi-exponential model to verify that pre-stimulus autoinhibition is the main contributor to difference in fast and slow type responses.

4.0 RESULT AND DISCUSSION

4.1 KINETIC MODELING: BI-EXPONENTIAL (5 PARAMETERS)

We could fit evoked DA responses in both fast sites and slow sites with the bi-exponential model. We administered raclopride, recorded predrug and postdrug responses at stimulation length of 10 seconds, and applied hang-up correction. Each response is averaged (n=6 fast sites, n=7 slow sites). Figure 12 (A) shows that both predrug and postdrug data sets can each be modeled with a single set of parameters. The slow site postdrug response has both a higher DA maximum concentration and faster release rate when compared to the slow site predrug response. This agrees with the known effect of raclopride; it abolishes the slow component, making slow response looks more like fast response.

In the case of fast domain (Figure 12 (B), while the postdrug response fits very well, the model underestimates the initial fast component of the predrug response. This corresponds to our previous findings that the parameters of the best model fit depends greatly on the fast and slow components of a single evoked DA response, and we can model the initial fast component individually as well (Walters et al., 2014). As the duration of the stimulation increases, the kinetic parameters shift more towards the major component in a single response, which is the slow component in this case. Figure 12 (B) demonstrated that the bi-exponential model fit is closer in agreement to the slow component and the parameters are demonstrated in table 1.

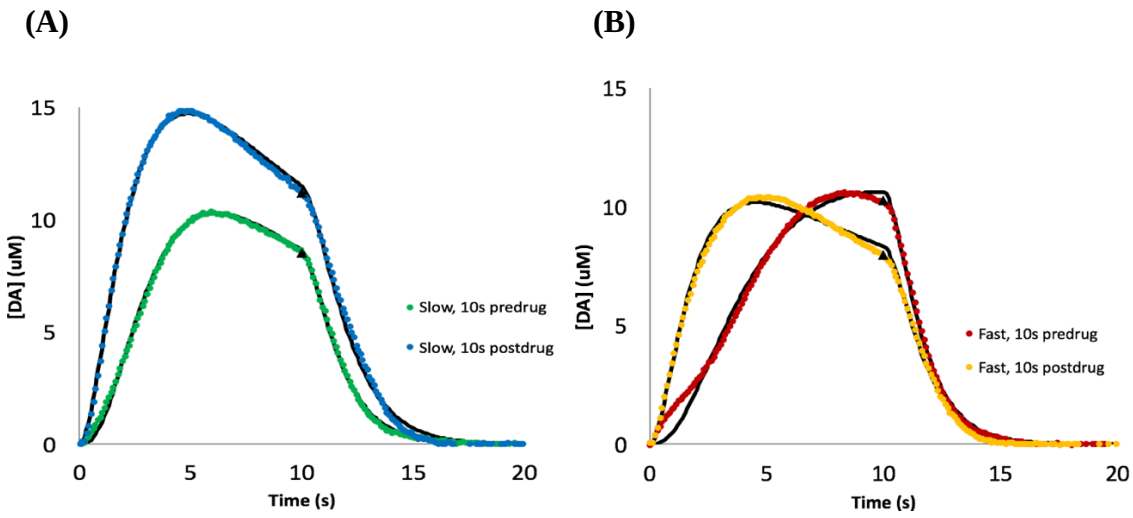

Figure 12 (A) Slow site and (B) fast site 10 seconds bi-exponential model fit.

SEMs omitted for clarity. Fast site n=6, slow site n=7.

Table 1. The parameters of bi-exponential model fit to 10 second data in fast and slow sites.

Parameter	Slow, 10s pre	Slow, 10s post	Fast, 10s pre	Fast, 10s post
R_p (mol)	5.10E-21	4.56E-21	1.72E-20	3.56E-21
k_T (s^{-1})	1.16	0.881	0.881	1.09
k_U (s^{-1})	1.17	0.874	1.65	1.09
k_{R1} (s^{-1})	0.084	0.072	0.092	0.053
k_{R2} (s^{-1})	0.632	18535	0.197	48.828

4.2 KINETIC HETEROGENEITY IN DIFFERENT SITES

The RD model is sufficient to fit 1 second and 3 seconds evoked responses. The relative fits and responses of slow type can be seen in figure 13 while fast type can be seen in figure 14. In both types of responses, the values of k_T do not have a set value, but we chose to report the parameter sets with k_T value ranges among 1-2. According to our previous report (Walters et al., 2015), the DA is being transported from the terminal to the electrode recording site at the same rate in both fast and slow domains and should not be changed based on pharmaceutical conditions. In other words, the difference between fast and slow domains are due to the kinetic effect instead of the physical space. However, the model has no ability to determine whether the rate determining step is transport or uptake and therefore the values are not within a range. This will be discussed in the later chapters.

Since raclopride makes slow type responses look more like fast type responses by increasing the initial release as well as the maximum DA concentration, the release per pulse parameter should be larger after the administration of raclopride. However, changes in parameters R_p and k_U between postdrug and predrug are not consistent in both fast and slow responses. This contradicts to what we observe in the evoked responses. The release per pulse parameter is coupled with the first order uptake rate because when one increases or decreases the other parameter responds in the same fashion. Moreover, the uptake occurs throughout the whole evoked response when DA is present. Therefore, looking at the parameters themselves is no longer sufficient; it is necessary to look at evoked responses in another way. The bi-exponential model is not only a more accurate way to fit longer responses, it also provides access to new information for both fast and slow components in one single evoked response.

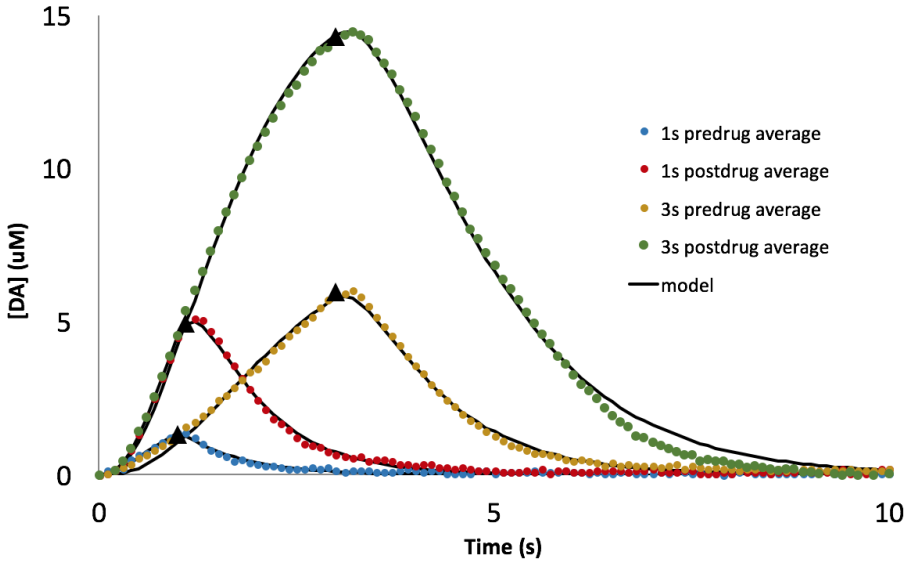

Figure 13 Slow site 1 second and 3 seconds evoked responses with RD model fits.

Average of n=7, SEMs omitted for clarity. T=0 s for start of the stimulus and triangles are the ends of the stimulus.

Table 2 The parameters of the RD model fit to the slow site 1 second and 3 seconds' data.

Parameter	Slow, 1s pre	Slow, 1s post	Slow, 3s pre	Slow, 3s post
R_p (mol)	3.82E-21	2.98E-21	2.97E-21	4.65E-21
k_T (s^{-1})	1.84	1.54	1.00	1.09
k_U (s^{-1})	21.46	3.53	5.37	1.09
k_R (s^{-1})	-1.40	-1.49	-0.53	-0.020

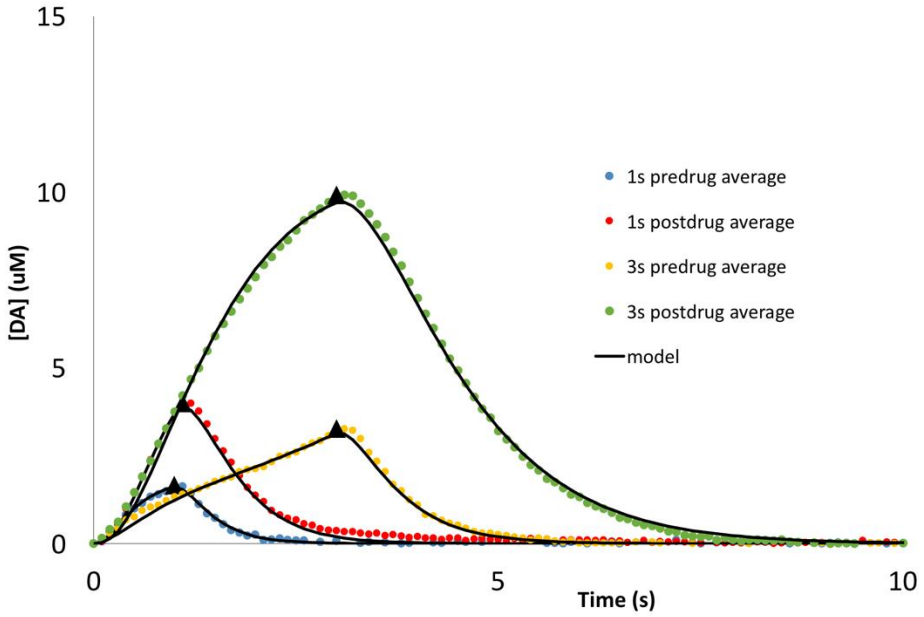

Figure 14 Fast site 1 second and 3 seconds evoked responses with RD model fits.

Average of n=6, SEMs omitted for clarity. t=0 s for start of the stimulus and triangles are the ends of the stimulus. The initial fast components of predrug overlap with the initial fast components of postdrug responses.

Table 3 The parameters of the RD model fit to the fast site 1 second and 3 seconds' data.

Parameter	Fast, 1s pre	Fast, 1s post	Fast, 3s pre	Slow, 3s post
R_p (mol)	2.57E-21	3.30E-21	1.50E-21	3.31E-21
k_T (s^{-1})	2.79	1.85	1.76	1.24
k_U (s^{-1})	6.55	4.29	3.80	1.24
k_R (s^{-1})	-0.38	-1.05	-0.35	-0.063

5.0 DELIVERY AND CLEARANCE CURVE

5.1 INTRODUCTION

The RD model uses first order kinetics to describe the rate of mass transport to the electrode and the rate of uptake from the electrode. As a result, the amount of DA delivered to and cleared from the area around the electrode depends on the concentration of DA in the inner and outer compartments. Therefore, we will compare the cumulative effect of the parameters, rather the individual parameters themselves. To this end, we calculated delivery (Equation 10) and clearance (Equation 11) plots with implementation of finite elements. The RD model can be expressed as the result of DA being simultaneously added to and removed from the area around the electrode:

Implementing finite element from the RD mathematical model:

$$\Delta DA_{ic} = R_p f e^{-k_r t} \Delta t - DA_{ic} k_T \Delta t$$

Equation 5

$$\Delta DA_{oc} = \frac{DA_{ic} k_T \Delta t}{V_{oc}} - [DA_{oc}] k_U \Delta t$$

Equation 6

$$DA_{IC,t+\Delta t} = DA_{ic,t} + \Delta_R\text{-}\Delta_T$$

Equation 7

$$DA_{oc,t+\Delta t} = DA_{oc,t} + \Delta_D\text{-}\Delta_C$$

Equation 8

The measured dopamine concentration can be represented as ΔDA:

$$\Delta DA = [DA]_{delivered}\text{-}[DA]_{cleared}$$

Equation 9

$$[DA]_{delivered} = \frac{DA_{ic}{}^{*}k_T{}^{*}\Delta t}{V_{oc}}$$

Equation 10

$$[DA]_{cleared} = [DA]_{oc}{}^{*}k_U{}^{*}\Delta t$$

Equation 11

Where $[DA]_{delivered}$ is the concentration of DA that reaches the outer compartment, $[DA]_{cleared}$ is the concentration of DA that is removed from the outer compartment, k_U is the first order uptake parameter, and $[DA]_{OC}$ is the concentration of DA in the outer compartment. Δt is a fixed small time element, Δ_R is the amount of DA released and Δ_T is the amount of DA transported to the outer compartment. These are used to evaluate the RD model by a finite element process. Data recorded in vivo was evaluated with the RD model as discussed previously using the number of parameters indicated, and the kinetic parameters from the best fits were used to construct the delivery and clearance curves.

5.2 DELIVERY AND CLEARANCE CHANGES OVER TIME

Fast-type responses exhibit an initially fast response to stimulation (within 0.2 seconds) that over time begins to slow. With the bi-exponential RD model and delivery and clearance curves as tools, we chose to investigate the origins of the fast-initial component of fast sites in detail. Stimulations of various lengths (180 pulses and 600 pulses, at 60 Hz) were applied, the responses were modeled with the bi-exponential RD model, and delivery curves were plotted.

As shown in figure 15 (A), in fast sites the delivery of both before and after raclopride increase immediately upon stimulation, except for the 10 second pre-drug stimulation. In this case, since the bulk of the stimulation is made up of the slow component, the model "ignores" the fast component to fit the bulk of the signal, underestimating the beginning of the curve (figure 12 (B) to minimize the sum of squared residuals (SSR). The beginning of the delivery curve reflects this underestimation. For the 3 second pre-drug and post-drug stimulations, the initial delivery of the first milliseconds remains the same, verifying that D2 antagonist has minimal effect to the fast component (Figure 12 (A).

Slow-type responses prior to drug administration tend to have the characteristic initial response delay in 3 and 10 second stimulations. After raclopride, however, this delay is eliminated, and DA is immediately delivered to the electrode. The slow site kinetics of DA delivery after raclopride exhibit characteristics of fast-type responses, confirming that differential activation of D2 receptors in fast and slow kinetic domains prior to stimulus onset is responsible for the varying responses to the stimulation.

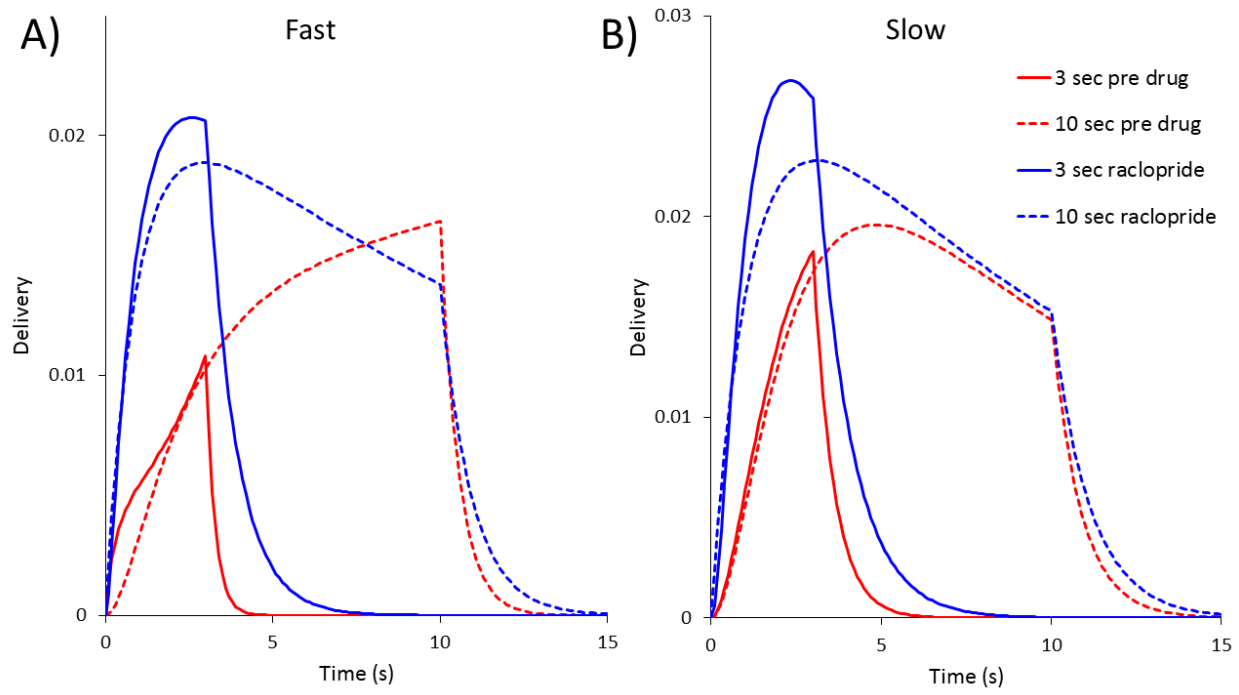

Figure 15 Delivery curves of 3 second and 10 second stimulations.

Before drug administration and post-raclopride in A) fast sites (n=6) and B) slow sites (n=7).

5.3 MULTIPLE PARAMETER SETS

In some cases, there are multiple equally good parameter sets to describe one single response, which can be verified by SSR and R^2 value. Based on the delivery and clearance curves created by different number of parameter sets, the responses can be categorized into 3 different types, which is discussed as follow.

The type A response has the simplest feature. As shown in figure 16 and figure 18, with linear rise during release and exponential fall after stimulation ends, it can be described with 3 parameters (R_p, $k_T = k_U$, k_R). In this specific case, with only 2 parameters (R_p, $k_T = k_U$) the model could produce either equally good fit with identical (Figure 17) or very close (Figure 19) delivery and clearance. Usually, there is only 1 best fit in this type of responses, with some occasions there are other "okay" fits.

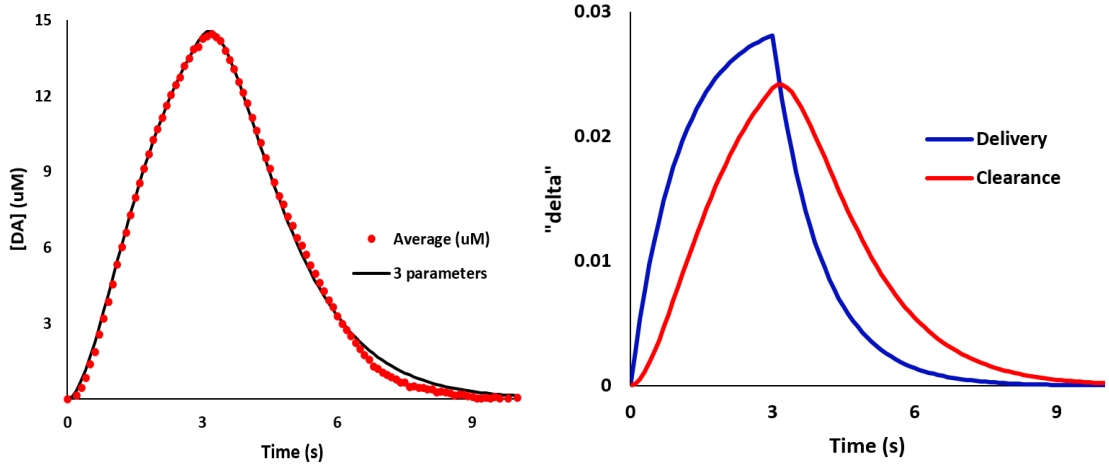

Figure 16 Delivery curves of slow-type 3 seconds stimulation after raclopride administration.

Left: showing the average response and 3-parameter fit. **Right:** showing the relative delivery and clearance curves. (3 parameter: n=7, R_p =4.65E-21, $k_U = k_T = 1$, k_R = -0.02, $r^2 > 0.9994$)

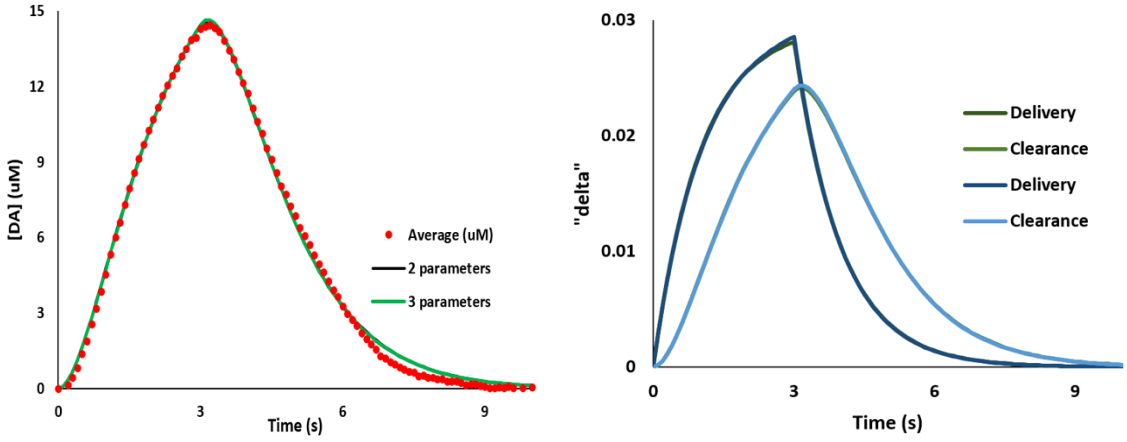

Figure 17 Delivery curves of slow-type 3 seconds stimulation after raclopride administration.

Left: showing both 2-parameter and 3-parameter versions create equally good fits. **Right:** showing the relative delivery and clearance curves overlap as well (2 parameter: n=7, R_p = 4.78E-21, $k_U = k_T = 0.99$, r^2>0.9994)

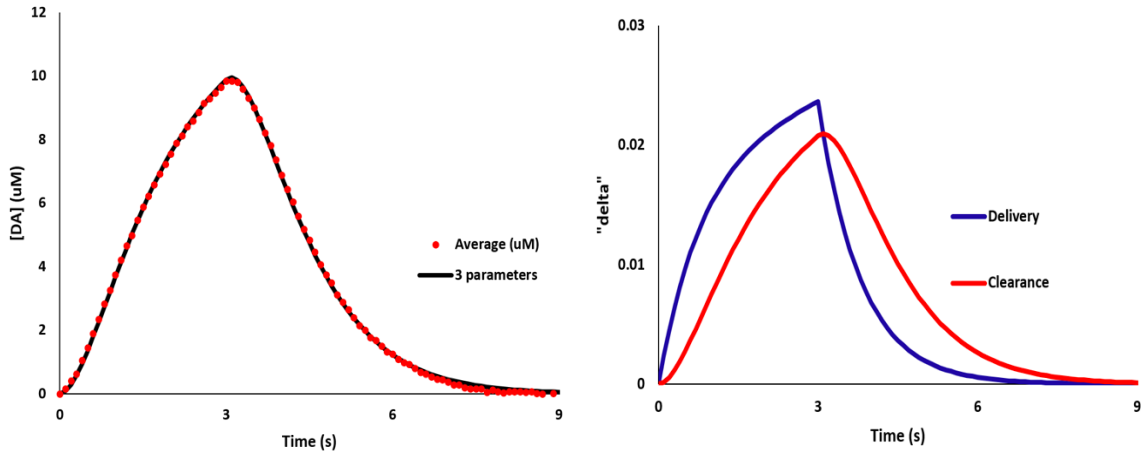

Figure 18 Delivery curves of fast-type 3 seconds stimulation after raclopride administration.

Left: showing the average response and 3-parameter fit.

Right: showing the relative delivery and clearance curves. (3 parameter: n=6, R_p =3.31E-21, k_U = k_T = 1.24, k_R = -0.063, $r^2 > 0.9999$)

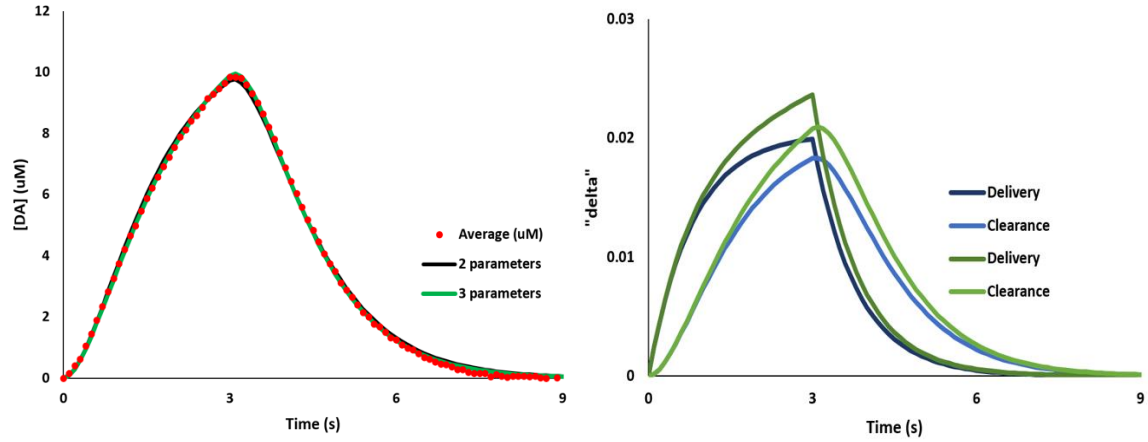

Figure 19 Delivery curves of slow-type 3 seconds stimulation after raclopride administration.

Left: showing both 2-parameter and 3-parameter versions create equally good fits.

Right: showing the relative delivery and clearance curves are very close (2 parameter: n=6, R_p = 3.56E-21, k_U = k_T = 1.20, r^2>0.9997)

The restricted diffusion model can produce two adjustable parameter sets in some responses, we categorize these responses as type B. The two parameter sets have interchangeable numerical values of k_T and k_U with identical value of k_R. Since R_p parameter tracks k_U, these two parameters would increase or decrease together. In this case, the model can produce identical fits when faster release is paired with slower transport and when slower release is paired with faster transport. The model cannot identify which is the rate-determining step. In this type of responses, the features are still relatively simpler with non-linear rise and exponential fall. While there are two best fits, based on the difference in parameter values, the delivery and clearance curves are different (Figure 20, figure 21 and figure 22).

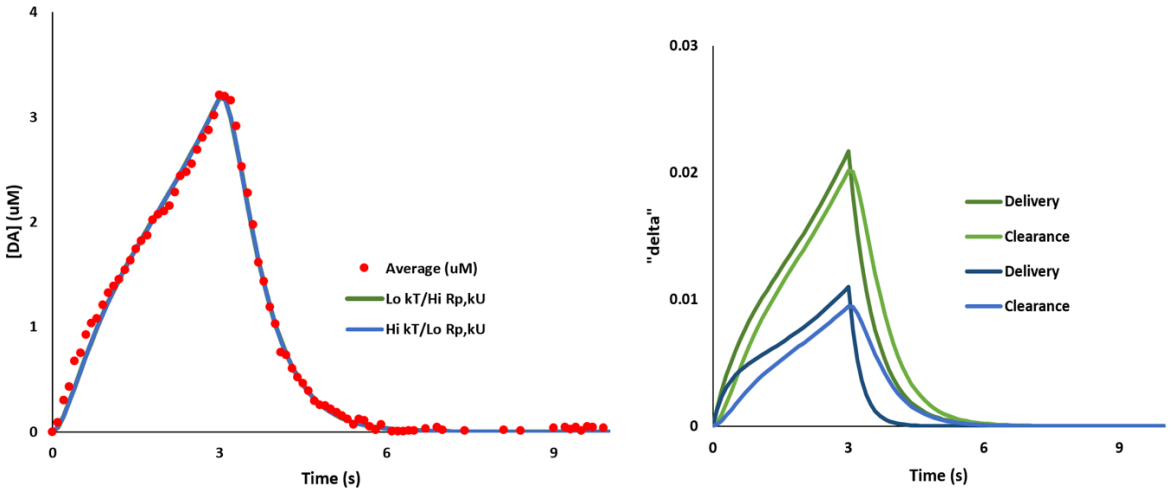

Figure 20 Delivery curves of fast-type 3 seconds stimulation.

Left: interchangeable numerical values of k_T and k_U versions create equally good fits.

Right: delivery and clearance curves of two best fits. (n=6, Green: R_p = 1.50E-21, k_U = 3.80, k_T = 1.76, k_R = -0.346, $r^2 > 0.9977$; Blue: R_p = 6.94E-22, k_U = 1.76, k_T = 3.80, k_R = -0.346, $r^2 > 0.9977$)

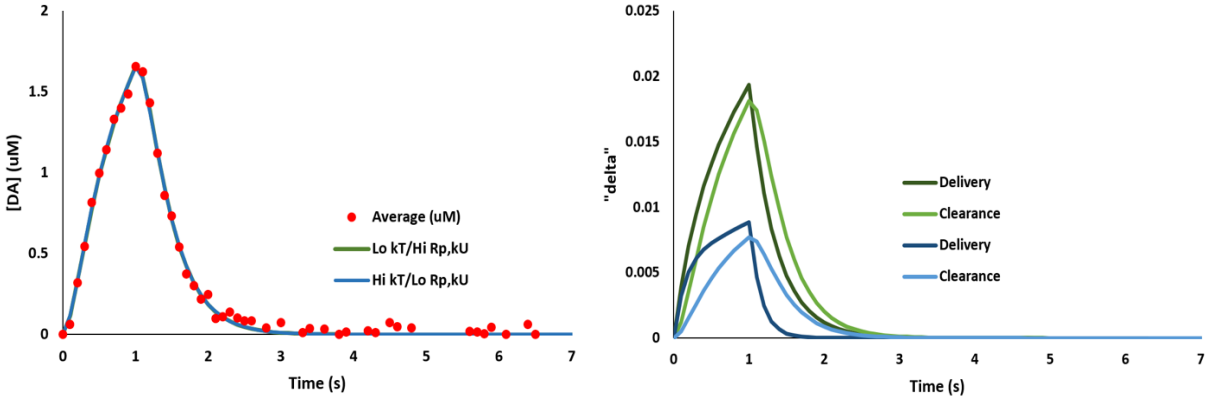

Figure 21 Delivery curves of fast-type 1 second stimulation.

Left: showing interchangeable numerical values of k_T and k_U versions create equally good fits. **Right:** delivery and clearance curves of two best fits. (n=6, 1: Green: R_p = 6.57E-21, k_U = 6.55, k_T = 2.79, k_R = -0.379, $r^2 > 0.9963$; Blue: R_p = 1.12E-21, k_U = 2.79, k_T = 6.40, k_R = -0.339, $r^2 > 0.9969$)

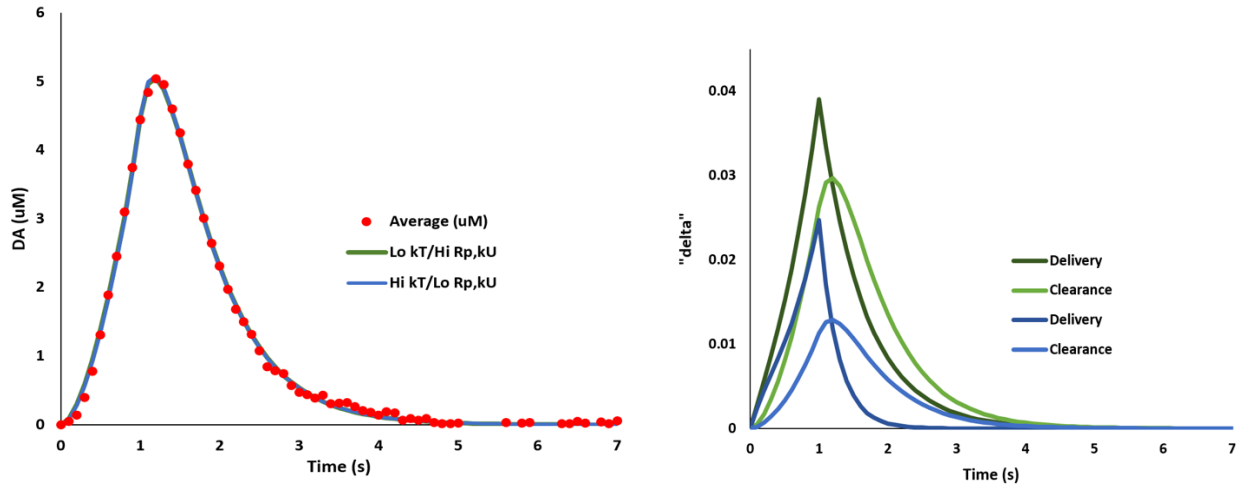

Figure 22 Delivery curves of fast-type 1 second stimulation after raclopride administration.

Left: showing interchangeable numerical values of k_T and k_U versions create equally good fits. **Right:** delivery and clearance curves of two best fits. (n=6, Green: R_p = 3.30E-21, k_U = 4.29, k_T = 1.85, k_R = -1.055, $r^2 > 0.9993$; Blue: R_p = 1.62E-21, k_U = 2.04, k_T = 3.62, k_R = -0.99, $r^2 > 0.9994$)

Because of its complex features containing non-linear rise and peaking during the stimulation instead of at the end of the stimulation, as well as the exponential fall, type C responses need 4 sometimes 5 variable parameters. Usually, responses with 10 seconds and longer stimulation lengths belong to this category and have 1 or more than 1 fits. With more parameters, we are capable of fitting more complex responses. Raclopride can eliminate the unneeded parameter because it can change slow type component to fast type, making the feature simpler. For example, in figure 23 and figure 25, we can tell that the extra parameter is not necessary. The k_{R1} value of the bi-exponential version has the same value as the 4-parameter version. With k_{R2} being such big number, the second release term of equation 3 would be zero. However, one should be cautious since the fits would lose their uniqueness. With a simpler feature, there can be more "best fits" to a certain evoked response. Therefore, our next step should be using the delivery and clearance curves to further interpret the necessity of increasing the total number of variable parameters.

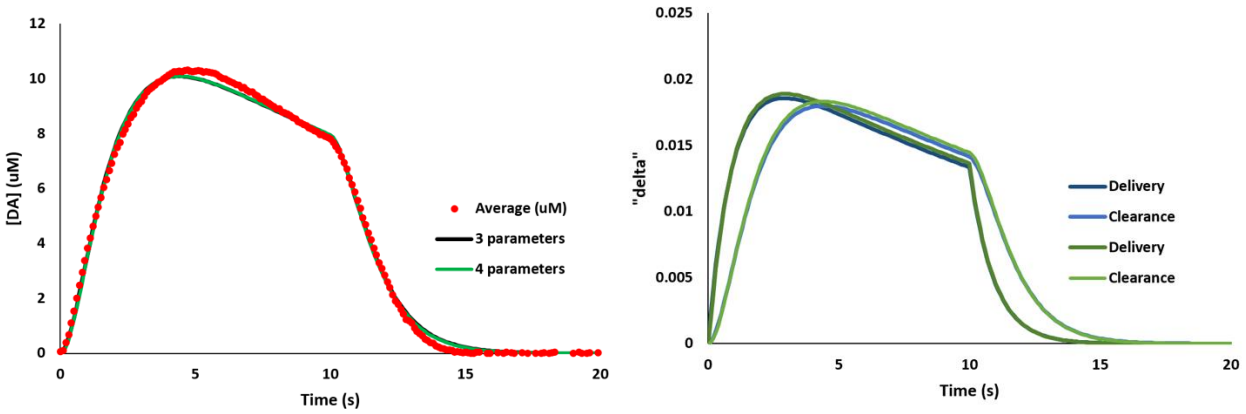

Figure 23 Delivery curves of fast-type 10 second stimulation after raclopride administration.

Left: showing both 4 or 5 parameters (in this case 3 or 4 parameters because $k_U = k_T$) create equally good fits.

Right: delivery and clearance curves of two best fits. (n=6, Green: R_p = 3.56E-21, $k_U = k_T$ = 1.09, k_{R1} = 0.053, k_{R2} = 48.83, $r^2 > 0.9992$; Blue: R_p = 3.50E-21, $k_U = k_T$ = 1.07, k_R = 0.054, $r^2 > 0.9992$)

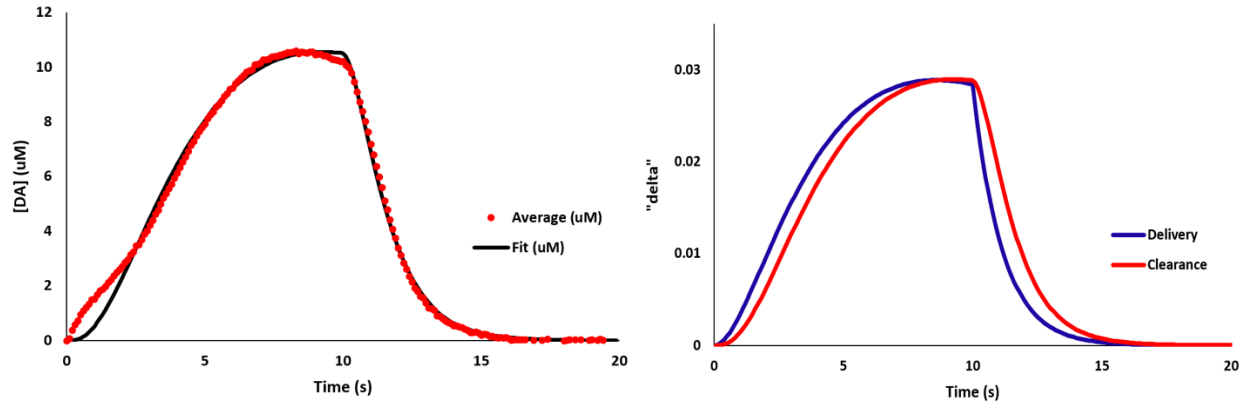

Figure 24 Delivery curves of fast-type 10 second stimulation.

Left: the only fit and requires 5 parameters. **Right:** delivery and clearance curves of the fit. (n=6, R_p = 1.72E-20, k_U = 1.65, k_T = 0.88, k_{R1} = 0.092, k_{R2} = 0.197, $r^2 > 0.9976$)

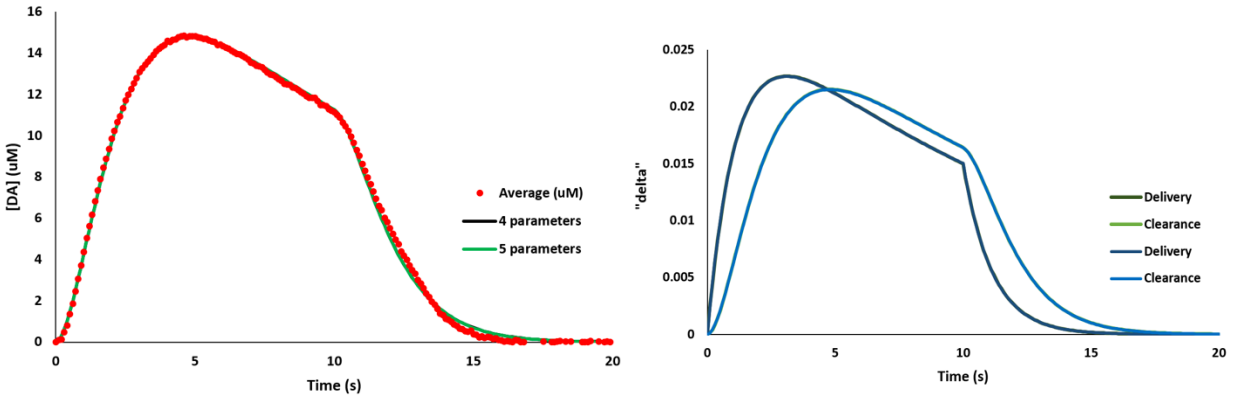

Figure 25 Delivery curves of slow-type 10 second stimulation after raclopride administration.

Left: showing both 4 or 5 parameters create equally good fits. **Right:** delivery and clearance curves of two best fits. (n=7, Green: R_p = 4.56E-21, $k_U = k_T$ = 0.88, k_{R1} = 0.072, k_{R2} = 18535, $r^2 > 0.9995$; Blue: R_p = 4.57E-21, $k_U = k_T$ = 0.88, k_R = 0.072, $r^2 > 0.9995$)

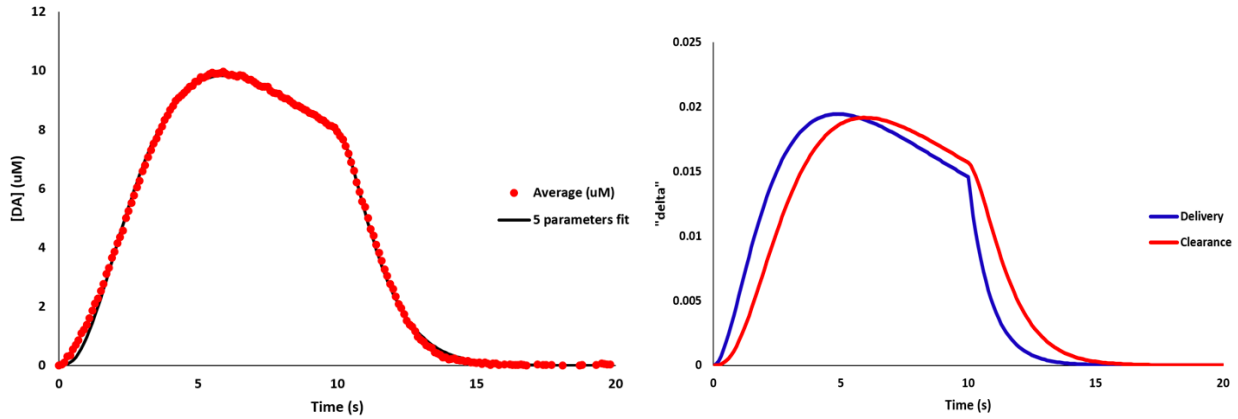

Figure 26 Delivery curves of slow-type 10 second stimulation.

Left: the only fit and requires 5 parameters. **Right:** delivery and clearance curves of the fit. (n=7, R_p = 5.10E-21, $k_U = k_T$ = 1.17, k_{R1} = 0.084, k_{R2} = 0.63, $r^2 > 0.9995$)

6.0 FUTURE DIRECTION

6.1 INVESTIGATE OTHER NEUROTRANSMITTERS

The bi-exponential model depicts the evoked dopamine responses well by being able to replicate the two-part release process. With this powerful tool in hand, we can study many other neurotransmitters in the central nervous system such as serotonin. In recent years, the possibility that serotonin acting in concert with DA contributes to schizophrenia and the action of antipsychotic drugs have received increasing attention (Adler et al., 1999; Howes and Kapur, 2009). The fact that a lot of anti-psychotic and anti-depression drugs are D2 antagonists makes studying this matter essential.

6.2 MODEL RESPONSES AT NEAR NEURON FIRING FREQUENCY

The stimulations being introduced in this document is at 60 Hz which is super-physiological. We would like to study responses at 30 Hz or even 15 Hz since the natural neuron burst firing rate is around 20 Hz (Cragg and Rice, 2004). With a combination of the bi-exponential model, delivery and clearance, we might be able to understand neuronal DA signals at rates closer to neuron firing, which can provide us with a physiologically-meaningful explanation of dopaminergic systems.

BIBLIOGRAPHY

Adler, L. E.; Freedman, R.; Ross, R. G.; Olincy, A.; Waldo, M. C. Elementary Phenotypes in the Neurobiological and Genetic Study of Schizophrenia. Biol. Psychiatry 1999, 46 (1), 8–18.

Bath, B. D.; Michael, D. J.; Trafton, B. J.; Joseph, J. D.; Runnels, P. L.; Wightman, R. M. Subsecond Adsorption and Desorption of Dopamine at Carbon-Fiber Microelectrodes. Anal. Chem. 2000, 72 (24), 5994–6002.

Benoit-Marand, M.; Jaber, M.; Gonon, F. Release and Elimination of Dopamine in Vivo in Mice Lacking the Dopamine Transporter: Functional Consequences. Eur. J. Neurosci. 2000, 12 (8), 2985–2992.

Benoit-Marand, M.; Borrelli, E.; Gonon, F. Inhibition of Dopamine Release via Presynaptic D2 Receptors: Time Course and Functional Characteristics in Vivo. J. Neurosci. 2001, 21 (23), 9134–9141.

Carr, G. D.; White, N. M. Contributions of Dopamine Terminal Areas to Amphetamine-Induced Anorexia and Adipsia. Pharmacol. Biochem. Behav. 1986, 25 (1), 17–22.

Ceccarelli, B.; Hurlbut, W. P. Vesicle Hypothesis of the Release of Quanta of Acetylcholine. Physiol. Rev. 1980, 60 (2), 396–441.

Cragg, S. J.; Rice, M. E. DAncing Past the DAT at a DA Synapse. Trends Neurosci. 2004, 27 (5), 270–277.

Delle Donne, K. T.; Sesack, S. R.; Pickel, V. M. Ultrastructural Immunocytochemical Localization of the Dopamine D2 Receptor within GABAergic Neurons of the Rat Striatum. Brain Res. 1997, 746 (1–2), 239–255.

Double, K. L.; Crocker, A. D. Dopamine Receptors in the Substantia Nigra Are Involved in the Regulation of Muscle Tone. Proc. Natl. Acad. Sci. U. S. A. 1995, 92 (5), 1669–1673.

Elsworth, J. D.; Roth, R. H. Dopamine Synthesis, Uptake, Metabolism, and Receptors: Relevance to Gene Therapy of Parkinson's Disease. Exp. Neurol. 1997, 144 (1), 4–9.

Ford, C. P. The Role of D2-Autoreceptors in Regulating Dopamine Neuron Activity and Transmission. Neuroscience 2014, 282, 13–22.

Garris, P. A.; Ciolkowski, E. L.; Pastore, P.; Wightman, R. M. Efflux of Dopamine from the Synaptic Cleft in the Nucleus Accumbens of the Rat Brain. J. Neurosci. 1994, 14 (10), 6084–6093.

Grace, A. A. The Tonic/phasic Model of Dopamine System Regulation: Its Relevance for Understanding How Stimulant Abuse Can Alter Basal Ganglia Function. Drug Alcohol Depend. 1995, 37 (2), 111–129.

Horvitz, J. C. Mesolimbocortical and Nigrostriatal Dopamine Responses to Salient Non- Reward Events. Neuroscience 2000, 96 (4), 651–656.

Howes, O. D.; Kapur, S. The Dopamine Hypothesis of Schizophrenia: Version III - The Final Common Pathway. Schizophr. Bull. 2009, 35 (3), 549–562.

Jaquins-Gerstl, A.; Michael, A. C. Comparison of the Brain Penetration Injury Associated with Microdialysis and Voltammetry. J. Neurosci. Methods 2009, 183 (2), 127–135.

Kile, B. M.; Walsh, P. L.; McElligott, Z. A.; Bucher, E. S.; Guillot, T. S.; Salahpour, A.; Caron, M. G.; Wightman, R. M. Optimizing the Temporal Resolution of Fast-Scan Cyclic Voltammetry. ACS Chem. Neurosci. 2012, 3 (4), 285–292.

Kita, J. M.; Parker, L. E.; Phillips, P. E. M.; Garris, P. A.; Wightman, R. M. Paradoxical Modulation of Short-Term Facilitation of Dopamine Release by Dopamine Autoreceptors. J. Neurochem. 2007, 102 (4), 1115–1124.

Lotharius, J.; Barg, S.; Wiekop, P.; Lundberg, C.; Raymon, H. K.; Brundin, P. Effect of Mutant α-Synuclein on Dopamine Homeostasis in a New Human Mesencephalic Cell Line. J. Biol. Chem. 2002, 277 (41), 38884–38894.

Michael, A. C.; Borland, L. M.; Mitala, J. J.; Willoughby, B. M.; Motzko, C. M. Theory for the Impact of Basal Turnover on Dopamine Clearance Kinetics in the Rat Striatum after Medial Forebrain Bundle Stimulation and Pressure Ejection. J. Neurochem. 2005, 94 (5), 1202–1211.

Missale, C.; Nash, S. R.; Robinson, S. W.; Jaber, M.; Caron, M. G. Dopamine Receptors: From Structure to Function. Physiol. Rev. 1998, 78 (1), 189–225.

Moquin, K. F.; Michael, A. C. Tonic Autoinhibition Contributes to the Heterogeneity of Evoked Dopamine Release in the Rat Striatum. J. Neurochem. 2009, 110 (5), 1491–1501.

Nesbitt, K. M.; Jaquins-Gerstl, A.; Skoda, E. M.; Wipf, P.; Michael, A. C. Pharmacological Mitigation of Tissue Damage during Brain Microdialysis. Anal. Chem. 2013, 85 (17), 8173–8179.

Onali, P.; Olianas, M. C.; Gessa, G. L. Characterization of Dopamine Receptors Mediating Inhibition of Adenylate Cyclase Activity in Rat Striatum. Mol. Pharmacol. 1985, 28, 138–145.

Pappatà, S.; Salvatore, E.; Postiglione, A. In Vivo Imaging of Neurotransmission and Brain Receptors in Dementia. J. Neuroimaging 2008, 18 (2), 111–124.

Peters, J. L.; Michael, A. C. Changes in the Kinetics of Dopamine Release and Uptake Have Differential Effects on the Spatial Distribution of Extracellular Dopamine Concentration in Rat Striatum. J. Neurochem. 2000, 74 (4), 1563–1573.

Reynolds, J. N.; Hyland, B. I.; Wickens, J. R. A Cellular Mechanism of Reward-Related Learning. Nature 2001, 413 (6851), 67–70.

Salahpour, A.; Ramsey, A. J.; Medvedev, I. O.; Kile, B.; Sotnikova, T. D.; Holmstrand, E.; Ghisi, V.; Nicholls, P. J.; Wong, L.; Murphy, K.; et al. Increased Amphetamine-Induced Hyperactivity and Reward in Mice Overexpressing the Dopamine Transporter. Proc. Natl. Acad. Sci. U. S. A. 2008, 105 (11), 4405–4410.

Schultz, W. Getting Formal with Dopamine and Reward. Neuron 2002, 36 (2), 241–263.

Taylor, I. M.; Nesbitt, K. M.; Walters, S. H.; Varner, E. L.; Shu, Z.; Bartlow, K. M.; Jaquins-Gerstl, A. S.; Michael, A. C. Kinetic Diversity of Dopamine Transmission in the Dorsal Striatum. J. Neurochem. 2015, 133 (4), 522–531.

Torres, G. E.; Gainetdinov, R. R.; Caron, M. G. Plasma Membrane Monoamine Transporters: Structure, Regulation and Function. Nat. Rev. Neurosci. 2003, 4 (1), 13–25.

Usiello, a; Baik, J. H.; Rougé-Pont, F.; Picetti, R.; Dierich, a; LeMeur, M.; Piazza, P. V; Borrelli, E. Distinct Functions of the Two Isoforms of Dopamine D2 Receptors. Nature 2000, 408 (November), 199–203.

Venton, B. J.; Zhang, H.; Garris, P. A.; Phillips, P. E. M.; Sulzer, D.; Wightman, R. M. Real-Time Decoding of Dopamine Concentration Changes in the Caudate-Putamen during Tonic and Phasic Firing. J. Neurochem. 2003, 87 (5), 1284–1295.

Walters, S. H.; Taylor, I. M.; Shu, Z.; Michael, A. C. A Novel Restricted Diffusion Model of Evoked Dopamine. ACS Chem. Neurosci. 2014, 5 (9), 776–783.

Walters, S. H.; Robbins, E. M.; Michael, A. C. Modeling the Kinetic Diversity of Dopamine in the Dorsal Striatum. ACS Chem. Neurosci. 2015, 6 (8), 1468–1475.

Walters, S. H.; Robbins, E. M.; Michael, A. C. The Kinetic Diversity of Striatal Dopamine: Evidence from a Novel Protocol for Voltammetry. ACS Chem. Neurosci. 2016.

Wang, Y.; Moquin, K. F.; Michael, A. C. Evidence for Coupling between Steady-State and Dynamic Extracellular Dopamine Concentrations in the Rat Striatum. J. Neurochem. 2010, 114 (1), 150–159.

Wightman, R. M.; Amatorh, C.; Engstrom, R. C.; Hale, P. D.; Kristensen, E. W.; Kuhr, W. G.; May, L. J. Real-Time Characterization of Dopamine Overflow and Uptake in the Rat Striatum. Neuroscience 1988, 25 (2), 513–523.

Wipf, D.; Wehmeyer, K. R.; Wightman, R. M. Disproportionation of Quinone Radical Anions in Protic Solvents at High. J. Org. Chem. 1986, 4 (Scheme I), 4760–4764.

Wu, Q.; Reith, M. E. A.; Wightman, R. M.; Kawagoe, K. T.; Garris, P. A. Determination of Release and Uptake Parameters from Electrically Evoked Dopamine Dynamics Measured by Real-Time Voltammetry. J. Neurosci. Methods 2001, 112 (2), 119–133.